Solar Energy 95 (2013) DOI: http://dx.doi.org/10.1016/j.solener.2013.01.021

Published in Solar Energy 95 (2013) pp. 376–391
www.elsevier.com/locate/solener
Received 29 September 2012; received in revised form 10 December 2012; accepted 12 January 2013
Available online 3 April 2013
http://dx.doi.org/10.1016/j.solener.2013.01.021

Estimation of background diffuse irradiance on orthogonal surfaces under partially obstructed anisotropic sky. Part I – Vertical surfaces

Stoyanka Marinova Ivanova*

University of Architecture, Civil Engineering and Geodesy, Sofia, Bulgaria

**Corresponding author: e-mail: solaria@online.bg*

Abstract:
This article presents an analytical approach to estimate the background component of diffuse irradiance on vertical surfaces under partially obstructed anisotropic sky, when neighbor orthogonal vertical and horizontal surfaces hide parts of the sky dome. This helps to calculate the incident diffuse radiation onto the façades of orthogonal buildings using defined here vertical and horizontal anisotropic sky view factors. The cases of infinitely long urban canyons and infinitely high vertical walls also are studied. The resulting equations include an isotropic part and an anisotropic correction. At last the article describes the fundamental relations between anisotropic sky view factors, which form base of anisotropic factor algebra.

***Keywords*:** Background diffuse irradiance; Obstructed anisotropic sky; Anisotropic view factor; Anisotropic factor algebra; Relations between anisotropic view factors; Infinite geometry

1. INTRODUCTION

The task of computing of incident solar energy on a building surface is important and not easy. The estimation of direct solar irradiance is relatively simple in comparison with the estimation of the incident diffuse irradiance. With the exception of clear skies, the diffuse irradiance is very often the dominant component of the global irradiance. Its precise estimation is important for all solar energy related work.

Most anisotropic models of the sky assume that the diffuse radiance can be represented by the superposition of two basic independent components – background component, which represents the dependence on air mass (as a function of the angle from the zenith) and another – circumsolar component, which represents the dependence on the scattering angle from the solar position.

A partial obstruction of the sky from other buildings or near walls happens very often. This paper aims to develop a method to estimate the incident diffuse irradiance on a surface under partially obstructed anisotropic sky. For this purpose the author of this paper analyses the most suitable anisotropic radiance and irradiance models and chooses Muneer's model as a base for further work. After a small modification in his model an approach is presented to estimate the background component of the diffuse irradiance on vertical surfaces under a partially obstructed sky, when the neighbor orthogonal vertical and/or horizontal surfaces hide part of the sky dome. For this purpose the author defines the concept of anisotropic sky view factor.

Solar Energy 95 (2013) DOI: http://dx.doi.org/10.1016/j.solener.2013.01.021

The last part of the article describes the fundamental relations between anisotropic sky view factors, which form the base of anisotropic factor algebra.

2. REQUIREMENTS TO THE ANISOTROPIC RADIANCE MODEL

In the beginning it is important to formulate the necessary requirements to the model, appropriate for an estimation of the irradiance on a slope under a partially obstructed sky:

(a) The model shall be able to predict the values of all components of diffuse radiance in any point of the sky.
(b) The model shall be in agreement with the measurements of the diffuse irradiance on a slope.
(c) The model shall cover the complete range of sky conditions from clear to dark overcast.
(d) The model shall be internally uncontroversial and balanced.

First two requirements dramatically decrease the number of suitable models. Most irradiance models (models proposed for calculating diffuse irradiance on a slope) do not fit, because they estimate the irradiance on slopes directly, and do not give information about the radiance of the sky. For example one of the most widely used anisotropic models is the model of **Perez et al. (1993)** which integrates three components – uniform background, circumsolar component and horizon brightening, represented as a line source at the horizon. This makes the model unsuitable for the cases when an obstruction hides top or bottom part of the sky towards a studied surface. The other problem is that the circumsolar and horizon brightness coefficients are a discontinuous step-function of sky conditions, the zenith angle and sky clearness and are obtained as table values.

The anisotropic model of **Muneer (1990)** avoids these problems. It is based on the formula of **Moon & Spencer (1942)** about the luminance distribution under overcast sky, on the work of **Kondratyev (1969)** about the similarity of luminance and radiance distribution – Eq. (1), and on the measurements and work of **Steven and Unsworth (1980)**.

$$R_\theta = R_z \frac{1 + b\cos\theta}{1 + b} \tag{1}$$

In this equation the radiance of a patch of an overcast sky $\boldsymbol{R_\theta}$ depends upon its zenith angle $\boldsymbol{\theta}$ (Fig. 1), the zenith radiance $\boldsymbol{R_z}$ and the radiance distribution index $\boldsymbol{b}$.

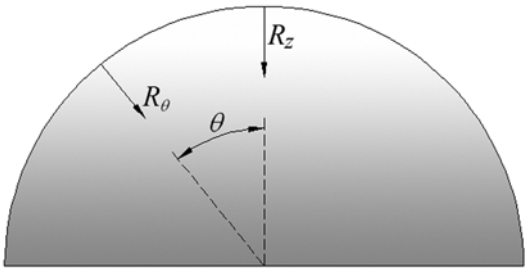

Fig. 1. A vertical view to a hemispherical sky with radiance distribution as described by Eq. (1)

Steven and Unsworth (1980) and later **Usher and Muneer (1989)** integrated Eq. (1) to obtain the ratio between the irradiance on inclined surface $\boldsymbol{I_{D\beta}}$ and the horizontal diffuse irradiance $\boldsymbol{I_{DH}}$ under overcast sky:

$$T = \frac{I_{D\beta}}{I_{DH}} = \cos^2\left(\frac{\beta}{2}\right) + \frac{2b}{\pi(3+2b)}\left[\sin(\beta) - \beta.\cos(\beta) - \pi.\sin^2\left(\frac{\beta}{2}\right)\right] \tag{2}$$

In the beginning this approach was developed only for overcast skies, but the measurements of Steven made it possible to expand it for non-overcast skies too. Thus the

Solar Energy 95 (2013) DOI: http://dx.doi.org/10.1016/j.solener.2013.01.021

resulting model was intended to be able to predict not only the irradiance on a slope, but also the radiance in every point of any sky. The radiance of a clear sky is described with negative values of the radiance distribution index b and thus the horizon radiance $R_h=R_{\pi/2}$ is bigger than the zenith's radiance $R_z=R_0$. For positive values of b the zenith's radiance R_z is bigger than the horizon radiance R_h, which is specific for an overcast sky. For b=0 the background component of the diffuse radiance can be considered as uniform for the whole sky dome.

The irradiance models of Perez et al. and Muneer are the most often used anisotropic models because of its results which place them among the top most accurate calculation irradiance models. This is reported by **Muneer (1990)**, **Loutzenhiser et al (2007)**, **Wlodarczyk & Novak (2009)**, **Evseev & Kudish (2009)**, etc. ESRA (European Solar Radiation Atlas) team selected the diffuse model of Muneer to use it as a base of PVGIS because of its sound theoretical basis and potential for later improvement (**Hofierka & Šúri, 2002**).

Most anisotropic models (Hay, Perez et al., Ma-Iqbal) assume all the circumsolar brightening concentrated at the position of the sun. When the sun is hidden by an object, but close to its edges, the radiance coming from the circumsolar region is not completely blocked in fact. Obviously this is a common disadvantage of these models.

The model of **Brunger and Hooper (1993)** overcomes this problem. It describes the radiance of every point in the sky dome in the form of a continuous function of angular position in the sky. The circumsolar radiance, which decreases rapidly with angular distance from the solar disk, is modeled as an exponential function of the angular distance between a sky segment and the sun. The air mass effect of horizon brightening is modeled with a cosine function, and the background component is modeled as uniform. The model is calibrated with the help of four coefficients; the recommended values of these coefficients are listed in a table according to the values of diffuse fraction K and clearness index K_t. This is an inconvenience and in combination with the difficult integration of the radiance function it makes the model too complicated to be used.

The author of this paper adopted some main principles of Muneer's model to estimate the background component of the diffuse irradiance on a slope under a partially obstructed sky. In this paper the circumsolar brightening is simplified as concentrated at the position of the sun, thus the circumsolar component is easy to be estimated.

3. EVALUATION AND MODIFICATION OF MUNEER'S MODEL

Muneer's model treats the shaded and sunlit surfaces separately and additionally distinguishes between overcast and non-overcast conditions of the sunlit surfaces.

3.1. Overcast conditions

In Muneer's model the slope diffuse irradiance $I_{D\beta}$ for surfaces in shade and sun-facing surfaces under overcast sky (with clearness index $K_t \leq 0.2$) is computed as:

$$I_{D\beta} = I_{HD} T \qquad (3)$$

where T is the ratio between the slope and horizontal irradiance, estimated with Steven's Eq. (2) as a function of b and slope angle β. For the European climate a shaded surface is modeled with b=5.73 and a sun-facing surface under overcast sky needs b=1.68. This diffuse radiance distribution model could be represented with the 3D-surface on Fig. 2a, where the outer circular edge represents the horizon, the center of each plot represents the zenith and the polar angle represents the azimuth angle. The specific data of this example are: Clearness index K_t=0.15; Diffuse to Global $K=D/G$=0.95; b_{south}=1.68; b_{north}=5.73; Solar zenith angle=35°; Zenith diffuse radiance R_z=67 W/m^2; Horizontal diffuse irradiance I_{DH} =160 W/m^2.

Solar Energy 95 (2013) DOI: http://dx.doi.org/10.1016/j.solener.2013.01.021

3.2. Non-overcast conditions

The diffuse irradiance on a sunlit surface under non-overcast sky is modeled as follows:

$$I_{D\beta} = I_{DH}\left[T(1-F) + F\,r_B\right] \quad (4)$$

where $\boldsymbol{F}$ is the ratio between the beam and the extraterrestrial horizontal irradiances ($F=B/E=(G-D)/E$), $\boldsymbol{T}$ is calculated as in Eq. (2), and $\boldsymbol{r_B}$=cos($\boldsymbol{i}$)/sin($\boldsymbol{h}$) is the beam conversion factor.

Non-overcast skies exhibit a continuously decreasing behavior of $\boldsymbol{b}$ and in **1990 Muneer** recommended the following equations obtained via data from 14 worldwide locations:

$$\frac{2b}{\pi(3+2b)} = 0.00333 - 0.415F - 0.6987F^2 \quad \text{for northern Europe} \quad (5a)$$

$$\frac{2b}{\pi(3+2b)} = 0.00263 - 0.712F - 0.6883F^2 \quad \text{for southern Europe} \quad (5b)$$

$$\frac{2b}{\pi(3+2b)} = 0.08000 - 1.050F - 2.8400F^2 \quad \text{for Japan} \quad (5c)$$

$$\frac{2b}{\pi(3+2b)} = 0.04000 - 0.820F - 2.0260F^2 \quad \text{for the globe} \quad (5d)$$

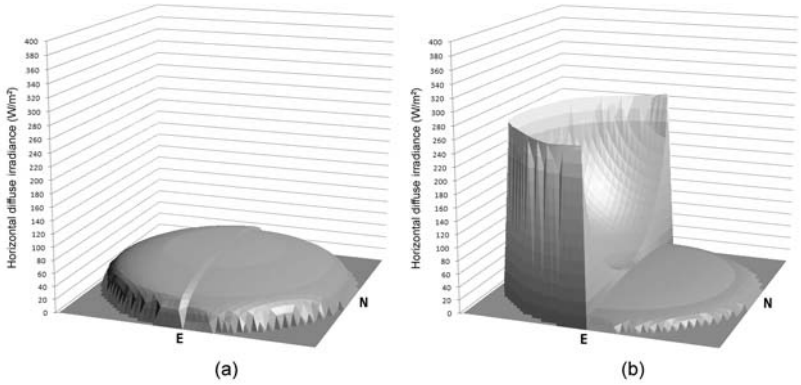

Fig. 2. Exemplary diffuse radiance distribution for Muneer's model: (a) overcast sky; (b) relatively clear sky. The outer circular edge represents the horizon, the center of each plot represents the zenith and the polar angle represents the azimuth angle.

Most of other models (**Hay, 1979**; **Hay and Davies, 1980**; **Hay and McKay, 1988**; Ma-Iqbal) accept that the background diffuse component is the same for sunlit and for shaded surfaces and use $\boldsymbol{F}$ (or other sky clarity index) as a value, which mixes the background and the circumsolar components. Muneer's model describes the diffuse irradiance on a shaded surface with the same equation as for shaded surface under overcast sky ($\boldsymbol{I_{D\beta} = I_{DH}\,T}$), where $\boldsymbol{T}$ depends by $\boldsymbol{b}$=5.73, even if this means the background radiance at the horizon is calculated of less value than background zenith radiance, which obviously is not true for a clear sky.

This separately treating of sunlit and shaded surfaces with different values of $\boldsymbol{b}$ leads to internal contradiction. If the receiving surface is horizontal or with a small slope angle, the irradiance coming from the both (southern and northern) halves of the sky dome has to be modeled with "sunlit" (negative) values of $\boldsymbol{b}$ – Eq. (5a – 5d). If the receiving surface is shaded, the same areas in the northern half of the sky dome has to be modeled with "shaded" (positive) value of $\boldsymbol{b}$=5.73.

Solar Energy 95 (2013) DOI: http://dx.doi.org/10.1016/j.solener.2013.01.021

Muneer and Zhang (2002) developed a mathematical relationship between b and K_t as follows:

$$\frac{2b_1}{\pi(3+2b_1)} = 0.382 - 1.11K_t \quad \text{(for } K_t > 0.2 \text{ and for southern half of the sky dome)} \tag{6a}$$

$$\frac{2b_2}{\pi(3+2b_2)} = 0.166 + 0.105K_t \quad \text{(for } K_t > 0.2 \text{ and for northern half of the sky dome)} \tag{6b}$$

For $K_t \le 0.2$, $b_1 = b_2 = 1.68$ after **Muneer (1990)**.

The value of $K_t > 0.2$ determines two different values of radiance distribution index b_1 and b_2. The diffuse irradiance on a horizontal surface I_{DH} can be estimated as:

$$I_{DH} = \frac{\pi R_z}{6}\left(\frac{3+2b_1}{1+b_1} + \frac{3+2b_2}{1+b_2}\right) \tag{7}$$

The circumsolar component cannot be seen in Eq. (7). Obviously its real value is included into the value of the background diffuse irradiance $\pi R_z(3+2b_1)/[6(1+b_1)]$ from the southern half of the sky dome. An illustration of exemplary diffuse radiance distribution as it follows from the values of b_1 and b_2 is on Fig. 2b. The specific data of this example are: Clearness index K_t=0.75; Diffuse to Global K=D/G=0.25; Solar zenith angle=35°; Beam to Extraterrestrial F=0.5625; b_1=-0.88; b_2=5; I_{DH} = 210 W/m^2; Zenith diffuse radiance R_z=32.2 W/m^2, calculated as follows from Eq. (7).

Muneer's model does not distinguish very clearly the background and circumsolar components. In his earlier publications (**Muneer, 1990, p. 157**) the background component of the diffuse slope irradiance $I_{BD\beta}$ was defined as $I_{BD\beta} = I_{DH}[T(1 - F)]$, but later he accepted to estimate it with $I_{BD\beta} = I_{DH} T$ and then the circumsolar radiance component to a sunlit surface follows to be $I_{CD\beta} = I_{DH}$ F $(r_B - T)$. Obviously he has his reasons for this, but it makes impossible to determine the values of the background and circumsolar components of the horizontal diffuse irradiance, when $T = 1$ and $r_B = 1$ and the calculated circumsolar horizontal diffuse irradiance I_{CDH} has to be zero as it follows from the Eq. (7) too. Even though as a sum of the background and circumsolar components the diffuse irradiance is correct, the radiance of any point of the sky corresponding to these components is not predicted correctly. Because of this in its current form Muneer's model can be evaluated mainly as an irradiance model, not as a correct radiance model.

3.3. Modification of Muneer's model for shaded surfaces under non-overcast skies

In spite of the mentioned problems Muneer's model contains many useful ideas and can be easily modified into a radiance model, suitable for our task. Actually it needs only two small changes: (1) redefinition of the background and circumsolar diffuse radiance in their usual meaning of independent components (as they were in Muneer's earlier articles); and from that position: (2) a different approach to the shaded surfaces.

First of all we have to distinguish the background and circumsolar components. As it was mentioned before, most other models use F (or other sky clarity index) as a parameter, which mixes the background and circumsolar components. If we apply this approach to Muneer's model we will receive the following equations for the background and circumsolar components of diffuse irradiance on a sloped surface:

$$I_{BD\beta} = I_{DH}(1-F)T = I_{DH}(1-F)\left\{\cos^2\left(\frac{\beta}{2}\right) + \frac{2b}{\pi(3+2b)}\left[\sin(\beta) - \beta.\cos(\beta) - \pi.\sin^2\left(\frac{\beta}{2}\right)\right]\right\} \tag{8}$$

$$I_{CD\beta} = I_{DH} F.r_B \tag{9}$$

Solar Energy 95 (2013) DOI: http://dx.doi.org/10.1016/j.solener.2013.01.021

For a horizontal surface (T=1 and r_B=1) under an unobstructed sky the background and the circumsolar components of the diffuse irradiance are estimated as follows:

$$I_{BDH} = I_{DH}(1-F) \quad (10)$$

$$I_{CDH} = I_{DH}F \quad (11)$$

The received diffuse irradiance on shaded surfaces has only a background component, while the sunlit surfaces receive both components (background and circumsolar) of the diffuse irradiance.

A background diffuse radiance distribution is illustrated in Fig. 3a and b, as it has to be expected from Eq. (10). The value of b is estimated, using Eq. (5a) for northern Europe. The value of the zenith background radiance R_z is estimated with Eq. (12) as follows:

$$R_z = I_{BDH}\frac{3(1+b)}{\pi(3+2b)} = I_{DH}(1-F)\frac{3(1+b)}{\pi(3+2b)} \quad (12)$$

An approximate 3D-modeling of circumsolar radiance with a summary value according to Eq. (10) is added to check the resulting forms of the diffuse radiance isopleths (Fig. 3b and c). The specific data of this example are: Clearness index K_t=0.75; Diffuse to Global K=D/G=0.25; Solar zenith angle=35°; Beam to Extraterrestrial F=0.5625; Horizontal diffuse irradiance I_{DH} = 210 W/m^2; Background horizontal diffuse component I_{BDH} = 92 W/m^2; Circumsolar horizontal diffuse component I_{CDH} = 118 W/m^2; Zenith background diffuse radiance R_z = 8.5 W/m^2; b = –0.88.

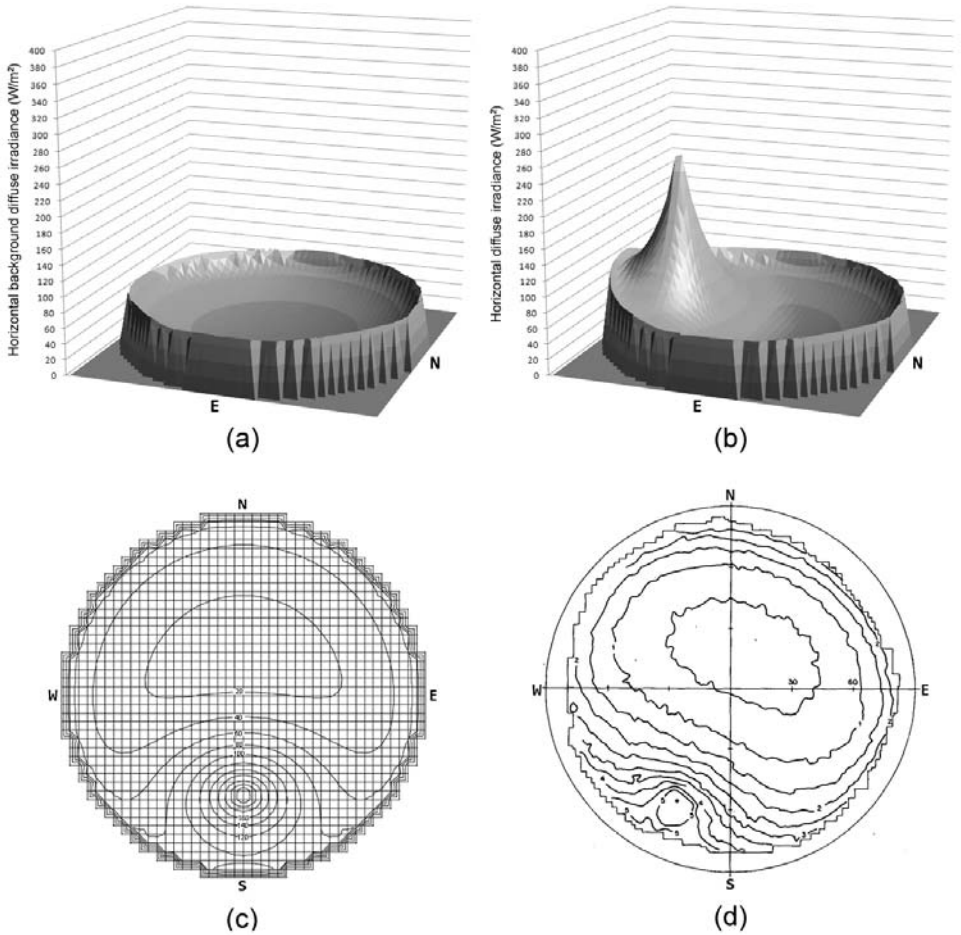

Fig. 3. Exemplary background & circumsolar diffuse radiance distribution for a model of a relatively clear sky: (a) 3D radiance distribution of background diffuse component; (b) 3D radiance distribution of

Solar Energy 95 (2013) DOI: http://dx.doi.org/10.1016/j.solener.2013.01.021

background and circumsolar diffuse components, solar zenith angle: 35°; (c) 2D radiance distribution; (d) radiance distribution as produced from photographic negatives (**McArthur & Hay, 1981**), solar zenith angle 61°

A vertical shaded surface receives only the background component of the diffuse irradiance estimated as follows:

$$I_{BDV} = I_{BDH}\left(0.5 + \frac{2b}{\pi(3+2b)}(1-\pi/2)\right) = I_{DH}(1-F)\left(0.5 + \frac{2b}{\pi(3+2b)}(1-\pi/2)\right) \quad (13)$$

For northern Europe and F=0.5625 the diffuse irradiance on a shaded vertical surface shall be:

$$I_{BDV} = I_{DH}(1-F)\left[0.5 + \left(0.00333 - 0.415F - 0.6987F^2\right)(1-\pi/2)\right] = 0.331 * I_{DH} \quad (14)$$

The estimated ratio of vertical diffuse irradiance to horizontal diffuse irradiance in this case is 0.331, which is very close to the measured data for European sites. Anyway this ratio varies daily and hourly as it is a function of the ratio between the beam and the extraterrestrial horizontal irradiances F (Fig. 4b). For northern Europe (Vaerloese, Denmark) Muneer presented such graphic of the ratio of vertical diffuse irradiation to horizontal diffuse irradiation (Fig. 4a):

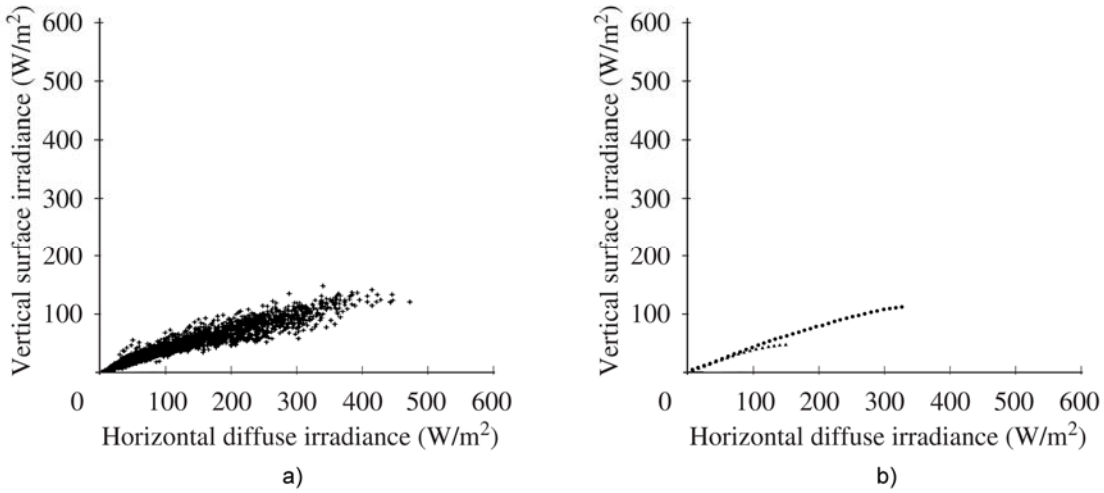

Fig. 4. Relationship between shaded vertical surface irradiation and horizontal diffuse irradiation: (a) Vaerloese data, graphic after **Muneer (1990)** and **Muneer (2004)**; (b) calculated values for clear sky and overcast sky after the modified model

If C_{ac} (coefficient of the anisotropic correction) according the geographic position is equal of the right side of Eq. (5a-5d), then the radiance distribution index b can be estimated as follows:

$$b = \frac{3\pi C_{ac}}{2 - 2\pi C_{ac}} = 1.5\frac{1}{\frac{1}{\pi C_{ac}} - 1} \quad (15)$$

As in the example above it is still possible from the parameters in Eqs. (5a)–(5d), (6a) and (6b) to estimate too small values of b (too close to -1). Value of b = -0.88 is equivalent of ratio R_h / R_z = 8.3 and indicates overestimated horizon brightening. It seems the modified model will need additional calibration – new parameters for Eqs. (5a)–(5d), (6a) and (6b).

The recommended modification of Muneer's model concerns only the calculation of the diffuse irradiance on horizontal or sloped shaded surfaces. In the same time it allows to estimate both components of the diffuse radiance for any point of the sky dome and thus the

Solar Energy 95 (2013) DOI: http://dx.doi.org/10.1016/j.solener.2013.01.021

modified model is appropriate to be used for estimating the irradiance on a surface under a partially obstructed sky.

4. DEFINITION OF ANISOTROPIC VIEW FACTOR – VERTICAL AND HORIZONTAL. CASE WITH UNOBSTRUCTED SKY

In order to predict the incident background diffuse solar radiation on a building with complex shape, we need to estimate it for any of its external surfaces. Most of them are vertical and horizontal and very often orthogonal. When we know the horizontal diffuse irradiance, we easy can find its background component, using Eq. (10). Later our task is to find the ratio between the background diffuse irradiance from a partially obstructed anisotropic sky onto the building's surfaces and the background horizontal diffuse irradiance from an unobstructed anisotropic sky. We will name this ratio **anisotropic background sky view factor** (horizontal, vertical and sloped).

As the orthogonal buildings are predominant, we will pay attention especially to the anisotropic sky view factors to orthogonal vertical and horizontal rectangular surfaces.

For a vertical surface ($\boldsymbol{\beta} = \boldsymbol{\pi}/2$) Eq. (13) about the ratio between vertical background component and horizontal background component of the diffuse irradiance leads to:

$$\frac{I_{BDV}}{I_{BDH}} = 0.5 + \frac{2b}{\pi(3+2b)}\left(1-\frac{\pi}{2}\right) = \frac{3\pi+4b}{2\pi(3+2b)} \tag{16}$$

It is useful to note that for $\boldsymbol{b}$=0 this distribution model of the background component of diffuse radiance becomes isotropic (uniform).

Let us consider an unobstructed anisotropic sky with nonzero $\boldsymbol{b}$ in order to estimate the background component of diffuse irradiance on a horizontal surface as a function of zenith radiance $\boldsymbol{R_z}$ and radiance distribution index $\boldsymbol{b}$.

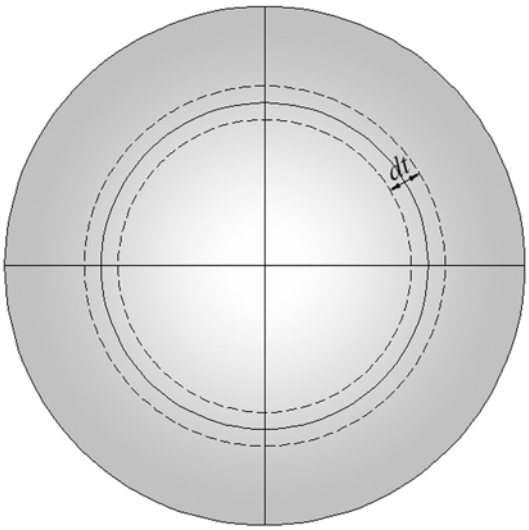

Fig. 5. Horizontal stereographic projection of a hemispherical anisotropic sky; the sky projection area is presented as a sum of concentric rings with circumference $\boldsymbol{l}$ and width $\boldsymbol{dt}$, situated around the sky's zenith

The stereographic projections are very useful in understanding the meaning of the sky view factor – for skies with uniform (isotropic) or anisotropic background radiance.

A stereographic projection is a projection of a sphere onto a plane. If we project the sky dome onto a horizontal plane, the projection is a unit circle (with radius $\boldsymbol{R}$=1 and area $\boldsymbol{\pi}$)

Solar Energy 95 (2013) DOI: http://dx.doi.org/10.1016/j.solener.2013.01.021

– Fig. 5. The ratio between the area of a stereographic projection of sky segment and π is the sky view factor of this segment under a sky with uniform background radiance.

The background diffuse irradiance I_{BDH}, which comes from the entire sky to a point on a horizontal surface, is the sum of the quantities of background diffuse radiance coming from the multitude of concentric rings with circumference l and width dt, situated around the sky's zenith (Fig. 5). If the hemispherical sky has a horizontal stereographic projection as a circle with R=1 then Eqs. (17) and (18) easily follow:

$$l = 2\pi \sin\theta \tag{17}$$

$$dt = \cos\theta . d\theta \tag{18}$$

Let us integrate the incident irradiance from the entire sky – Eq. (19):

$$I_{BDH} = \int_0^{\pi/2} R_\theta . l . dt = \int_0^{\pi/2} R_z \frac{1 + b.\cos\theta}{1+b} 2\pi . \sin\theta . \cos\theta . d\theta = \frac{2\pi R_z}{1+b} \int_0^{\pi/2} \sin\theta . \cos\theta . (1 + b.\cos\theta) d\theta \tag{19}$$

$$I_{BDH} = R_z \frac{\pi(3+2b)}{3(1+b)} \tag{20}$$

By analogy the background diffuse irradiance I_{BDV}, coming from an unobstructed sky to a point on a vertical surface, is calculated as the sum of the quantities of background diffuse radiance coming from multitude of horizontal bands with length l and width dt, situated between the horizon and zenith (Fig. 6).

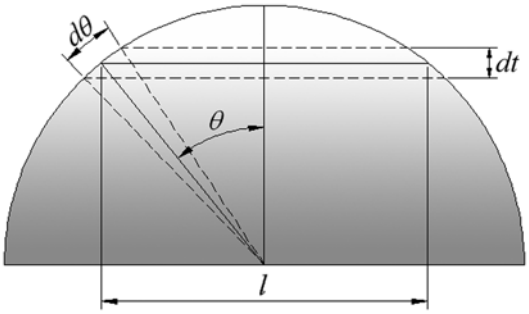

Fig. 6. Vertical stereographic projection of a hemispherical anisotropic sky; the projection on a vertical surface of a concentric sky ring around the sky's zenith with zenith angle θ and width $d\theta$ can be represented as a horizontal band with width l and height dt

If we project the sky dome to a point of a vertical plane, the stereographic projection will be a unit semicircle (with radius R=1 and area π/2), then:

$$l = 2\sin\theta \tag{21}$$

$$dt = \sin\theta . d\theta \tag{22}$$

This way we receive a definite integral in order to estimate the background component of the diffuse irradiance on a vertical surface:

$$I_{BDV} = \int_0^{\pi/2} R_\theta . l . dt = \int_0^{\pi/2} R_z \frac{1 + b.\cos\theta}{1+b} 2\sin\theta . \sin\theta d\theta = \frac{2R_z}{1+b} \int_0^{\pi/2} \sin\theta . \sin\theta . (1 + b.\cos\theta) d\theta \tag{23}$$

$$I_{BDV} = R_z \frac{(3\pi + 4b)}{6(1+b)} \tag{24}$$

Solar Energy 95 (2013) DOI: http://dx.doi.org/10.1016/j.solener.2013.01.021

Let us name the ratio between vertical background diffuse irradiance from an anisotropic sky and horizontal background diffuse irradiance from an unobstructed anisotropic sky, **anisotropic background vertical sky view factor**, or for short **anisotropic vertical factor** *(AVF)*. For an unobstructed sky it is estimated as:

$$AVF = \frac{I_{BDV}}{I_{BDH}} = \frac{R_z \dfrac{(3\pi + 4b)}{6(1+b)}}{R_z \dfrac{\pi(3+2b)}{3(1+b)}} = \frac{3\pi + 4b}{2\pi(3+2b)} \tag{25}$$

The resulting Eq. (25) for the maximum possible value of the anisotropic vertical factor is equivalent to Eq. (16).

5. BASIC ANISOTROPIC VERTICAL FACTORS FROM A PARTIALLY OBSTRUCTED SKY TO A POINT

Let us consider a rectangular cuboid (Fig. 7) – parallelepiped with dimensions ***a*** × ***c*** × ***d***. For our purpose we will examine some of the cuboid's walls as solid, and others – as completely transparent. Let us project the lines of the rectangular cuboid's edges stereographically to a point (or differential plane element) on one of the vertical walls, at distance ***x*** from the left vertical edge and at distance ***h*** from the top horizontal edge. In this way we receive the basic sectors which we will combine later to receive possible sky projections.

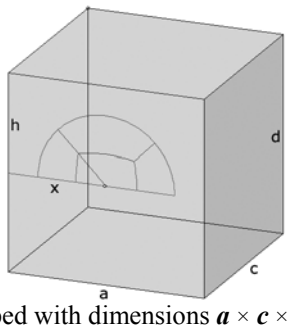

Fig. 7. Rectangular cuboid – parallelepiped with dimensions ***a*** × ***c*** × ***d***, with a stereographic projection onto a point on a cuboid's vertical wall. The point is at distance ***x*** from the left vertical edge and at distance ***h*** from the top horizontal edge of the studied vertical wall. The projections of the other lines of the cuboid's edges delimit the basic considered sky sectors

5.1. Anisotropic factors from the basic sky sectors to a point of vertical surface

Let the basic circular sectors in this stereographic projection have names starting with letter "A" and the basic elliptic sectors have names starting with letter "B" (Fig. 8).

Solar Energy 95 (2013) DOI: http://dx.doi.org/10.1016/j.solener.2013.01.021

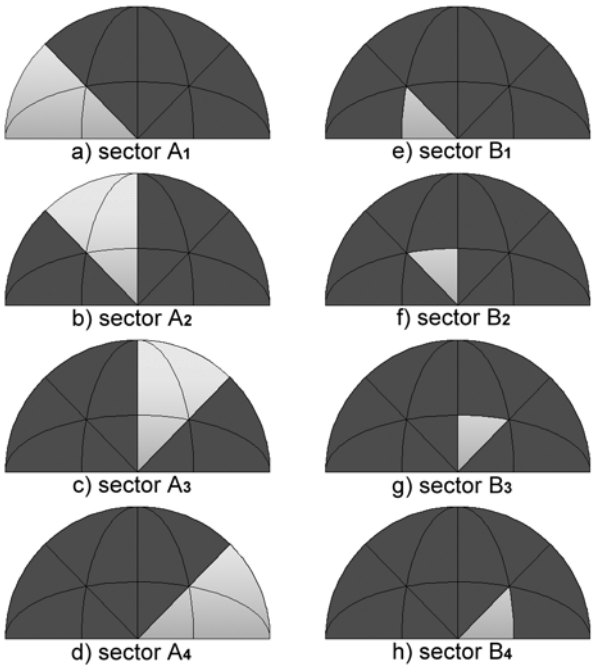

Fig. 8. Basic considered sectors: circular sectors $\boldsymbol{A_1}$, $\boldsymbol{A_2}$, $\boldsymbol{A_3}$, $\boldsymbol{A_4}$; elliptic sectors $\boldsymbol{B_1}$, $\boldsymbol{B_2}$, $\boldsymbol{B_3}$, $\boldsymbol{B_4}$

The vertical factor (*VF*) for unobstructed sky with uniform (isotropic) background diffuse component is 0.5. If a part of the sky is obstructed, then *VF* is estimated as a ratio between the area of stereographic projection of the visible part of the sky and the total area $\boldsymbol{\pi}$ of the unit circle with radius 1.

When we consider anisotropic sky, we have to take into consideration also the gradually changing radiance from the zenith to horizon – Eq. (1). For an overcast sky the background diffuse radiance is decreasing from the zenith to the horizon, and for a clear sky – it is increasing from the zenith to the horizon.

Let us consider the circular basic sector $\boldsymbol{A_1}$ (Fig. 8a) in the estimation of its anisotropic sky vertical factor (*AVF*). First we estimate the irradiance I_{A_1} from this sector using Eqs. (1), (21) and (22):

$$I_{A_1} = \int_{\pi/2-arctg\frac{h}{x}}^{\pi/2} R_z \frac{1+b.\cos\theta}{1+b}\sin\theta\left(\sin\theta - \frac{x\cos\theta}{h}\right)d\theta \tag{26}$$

The integration leads to:

$$I_{A_1} = \frac{R_z}{1+b}\left(\frac{1}{2}arctg\frac{h}{x} + \frac{b}{3}(1-\frac{x}{\sqrt{x^2+h^2}})\right) \tag{27}$$

As we defined the **anisotropic vertical factor** (*AVF*) as the ratio between vertical diffuse background irradiance and horizontal diffuse background irradiance from an anisotropic sky, so the *AVF* for the circular sector $\boldsymbol{A_1}$ will be estimated as the following ratio:

$$AVF_{A_1\to point} = \frac{I_{A_1}}{I_{BDH}} = \frac{\frac{R_z}{1+b}\left(\frac{1}{2}arctg\frac{h}{x} + \frac{b}{3}(1-\frac{x}{\sqrt{x^2+h^2}})\right)}{R_z\frac{\pi(3+2b)}{3(1+b)}} \tag{28}$$

Solar Energy 95 (2013) DOI: http://dx.doi.org/10.1016/j.solener.2013.01.021

The result is included as Eq. (A.1) in Appendix Table A.1. By analogy we estimate the *AVF* for the basic sectors $\boldsymbol{A_2}$, $\boldsymbol{B_1}$ and $\boldsymbol{B_2}$ resulting in the equations listed in the same Table A.1 as Eqs. (A.2) to (A.4). The values for the sectors $\boldsymbol{A_3}$, $\boldsymbol{A_4}$, $\boldsymbol{B_3}$, $\boldsymbol{B_4}$ we could estimate using the relevant equations for $\boldsymbol{A_2}$, $\boldsymbol{A_1}$, $\boldsymbol{B_2}$, $\boldsymbol{B_1}$.

5.2. Derivative anisotropic factors to a point of vertical surface

With combinations of sums and differences of the ***AVF*** of the mentioned basic sectors we can estimate the value of the ***AVF*** of each visible part of sky in cases when it is obstructed by an orthogonally orientated horizontal or vertical surface (Figs. 9 and 10).

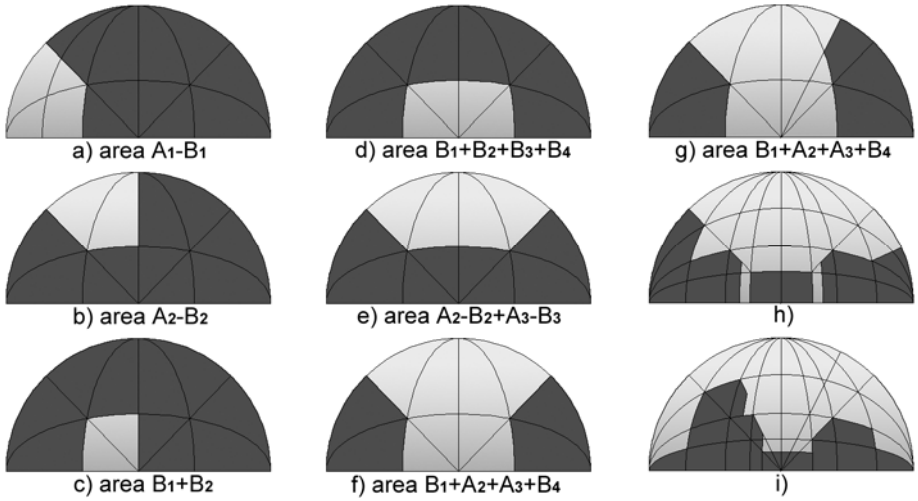

Fig. 9. Combined projections: a) area $\boldsymbol{A_1}$–$\boldsymbol{B_1}$; b) area $\boldsymbol{A_2}$–$\boldsymbol{B_2}$; c) area $\boldsymbol{B_1}$+$\boldsymbol{B_2}$; d) area $\boldsymbol{(B_1+B_2)+(B_3+B_4)}$; e) area $\boldsymbol{(A_2–B_2)+(A_3–B_3)}$; f) area $\boldsymbol{(B_1+A_2)+(A_3+B_4)}$; g,h,i) more complex projections

The stereographic projections on Fig. 9a to e look like interiors, but the estimated ***AVF*** for these areas could be subtracted from the maximum ***AVF*** for a vertical surface: $(3\pi+4b)/[2\pi(3+2b)]$. This way we receive the resulting value of ***AVF*** of the visible sky areas toward an exterior wall (façade) as in Fig. 9f, g, etc. This makes the method suitable for both interior (Fig. 10a) and exterior tasks (Fig. 10b and c).

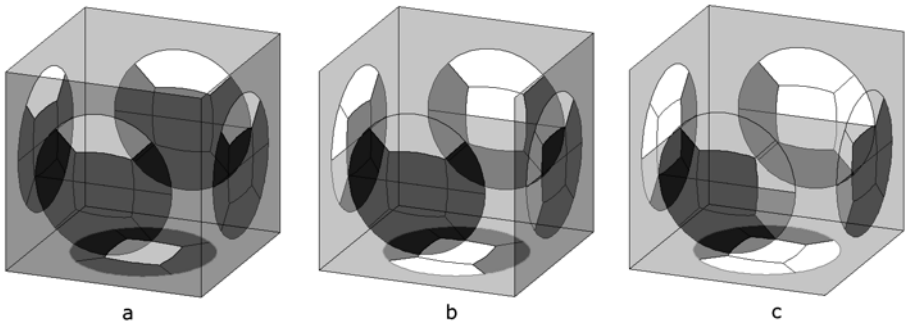

Fig. 10. Composite images of all stereographic projections on cuboid's surfaces, when only some of them are solid: a) 4 vertical walls and top opening; b) 3 vertical walls and two openings; c) 2 vertical walls and three openings

In Table 1 are listed the resulting equations (29) to (31) for ***AVF*** of the three most widely used combined projections: $\boldsymbol{A_1}$–$\boldsymbol{B_1}$, $\boldsymbol{A_2}$–$\boldsymbol{B_2}$, $\boldsymbol{B_1}$+$\boldsymbol{B_2}$.

Solar Energy 95 (2013) DOI: http://dx.doi.org/10.1016/j.solener.2013.01.021

Table 1. Equations for estimation of derivative anisotropic view factors of combined projections to a point of a vertical rectangle

Image of combined projection	Equation	Equation No
$A_1 - B_1$ 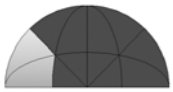	$AVF_{A_1-B_1\to point} = AVF_{A_1\to point} - AVF_{B_1\to point} =$ $= \frac{3}{3+2b}.\frac{1}{2\pi}\left(\text{arctg}\frac{h}{x} - \frac{x}{\sqrt{x^2+c^2}}\text{arctg}\frac{h}{\sqrt{x^2+c^2}}\right) +$ $+ \frac{2b}{3+2b}.\frac{1}{2\pi}\left(1 - \frac{x}{\sqrt{x^2+h^2}} - \frac{x}{\sqrt{x^2+c^2}} + \frac{x}{\sqrt{x^2+c^2+h^2}}\right)$	(29)
$A_2 - B_2$ 	$AVF_{A_2-B_2\to point} = AVF_{A_2\to point} - AVF_{B_2\to point} =$ $= \frac{3}{3+2b}.\frac{1}{2\pi}\left(\text{arctg}\frac{x}{h} - \frac{h}{\sqrt{c^2+h^2}}\text{arctg}\frac{x}{\sqrt{c^2+h^2}}\right) +$ $+ \frac{2b}{3+2b}.\frac{1}{2\pi}\left(\frac{x}{\sqrt{x^2+h^2}} - \frac{xh^2}{(c^2+h^2)\sqrt{x^2+c^2+h^2}}\right)$	(30)
$B_1 + B_2$ 	$AVF_{B_1+B_2\to point} = AVF_{B_1\to point} + AVF_{B_2\to point} =$ $= \frac{3}{3+2b}.\frac{1}{2\pi}\left(\frac{x}{\sqrt{x^2+c^2}}\text{arctg}\frac{h}{\sqrt{x^2+c^2}} + \frac{h}{\sqrt{c^2+h^2}}\text{arctg}\frac{x}{\sqrt{c^2+h^2}}\right) +$ $+ \frac{2b}{3+2b}.\frac{1}{2\pi}\left(\frac{x}{\sqrt{x^2+c^2}} - \frac{x}{\sqrt{x^2+c^2+h^2}} + \frac{xh^2}{(c^2+h^2)\sqrt{x^2+c^2+h^2}}\right)$	(31)

The resulting equations (29) – (31) include two parts:

a) The isotropic part multiplied by **3/(3+2*b*)** is the isotropic view factor for the specific sector.
b) The anisotropic part multiplied by **2*b*/(3+2*b*)** is an anisotropic correction of the isotropic view factor.

Thus the listed equations for $b = 0$ could be used for irradiance models (Perez, Hay, etc.), where the background component of the diffuse irradiance is uniform (isotropic).

5.3. Anisotropic factors from infinitely high or long shading surfaces to a point of vertical surface

The obstructing surfaces with infinitely large dimensions in horizontal or vertical directions are also interesting and useful to be studied.

On a stereographic vertical projection, let the basic sections with large Y axis have names starting with letter “C”, and the basic sections with large X axis have names starting with letter “D” (Fig. 11).

Solar Energy 95 (2013) DOI: http://dx.doi.org/10.1016/j.solener.2013.01.021

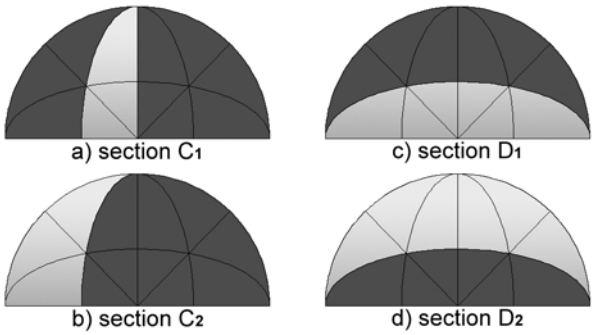

Fig. 11. Basic sections: a) Section $\boldsymbol{C}_1$; b) Section $\boldsymbol{C}_2$; c) Section $\boldsymbol{D}_1$; d) Section $\boldsymbol{D}_2$

C-sections are projections of the sky between infinitely high walls, ***D***-sections – projections of the sky above infinitely long canyons or under infinitely long shading devices. Using the same approach as for the previous equations, listed in Appendix Table A.1 we come to the integral in Eq. (32) and result in Eqs. (33) and (34).

$$I_{C_1} = \int_0^{\pi/2} R_z \frac{1+b.\cos\theta}{1+b} \sin\theta.\sin\theta.\frac{x}{\sqrt{x^2+c^2}} d\theta \tag{32}$$

$$I_{C_1} = \frac{R_z}{1+b}.\frac{x}{\sqrt{x^2+c^2}} \int_0^{\pi/2} \sin\theta.\sin\theta.(1+b.\cos\theta)d\theta = \frac{R_z.(3\pi+4b)}{12(1+b)}.\frac{x}{\sqrt{x^2+c^2}} \tag{33}$$

$$AVF_{C_1\to point} = \frac{I_{C_1}}{I_{DH}} = \frac{\frac{R_z \frac{x}{\sqrt{x^2+c^2}}(3\pi+4b)}{12(1+b)}}{\frac{R_z\pi(3+2b)}{3(1+b)}} = \frac{3\pi+4b}{4\pi(3+2b)}.\frac{x}{\sqrt{x^2+c^2}} \tag{34}$$

All resulting equations for sections $\boldsymbol{C}_1$, $\boldsymbol{C}_2$, $\boldsymbol{D}_1$, $\boldsymbol{D}_2$ are listed as Eq. (A.5) to (A.8) in Appendix Table A.2. There is a relationship between these equations and some equations in table A.1. For example Eq. (A.5) corresponds to Eq. (A.3) for infinitely large value of $\boldsymbol{h}$ ($\boldsymbol{h} \to \infty$), and Eq. (A.7) corresponds to Eq. (A.4), but for an infinitely large value of $\boldsymbol{x}$ ($\boldsymbol{x} \to \infty$).

The ***AVF*** from the visible sky area to a point on a vertical wall on Fig. 9h and 9i could be estimated as a combination of sums and differences between ***AVF*** to ***C***- and ***D***-sections and ***A***- and ***B***-sectors.

6. AVERAGE VALUE OF BASIC ANISOTROPIC VERTICAL FACTORS

To estimate the total quantity of the incident background diffuse irradiance from partially obstructed sky to a surface we first need to calculate the average value of anisotropic sky view factor to this surface. There could be three approaches for this:

The first approach is approximate and relatively easy. In this case we calculate the anisotropic sky factor for the centre point of the surface using the equations described in the previous section and listed in Appendix Tables A.1 and A.2. This usually leads to overestimated values.

Another version of this approach is SRDM – Sky Radiance Distribution Model (**Clarke et al, 2007**), it splits the sky into hundreds sky patches, determined by the altitude and azimuth of their centres. The intensity of the diffuse radiance from each of them is calculated. Shading is included by adding patch blockages, if a sky patch is obscured from

Solar Energy 95 (2013) DOI: http://dx.doi.org/10.1016/j.solener.2013.01.021

view by neighboring buildings toward the centre of the surface. The incident diffuse irradiance on the surface is calculated using integrated sky patch radiance and blockages.

The second approach is also approximate but more precise. The surface is divided in two perpendicular directions into many fragments with equal areas. Then the average value of anisotropic factors for the centre points of all fragments is estimated using the equations described in the previous sections. Through increasing the number of fragments we can improve the accuracy of the final result. SRDM in combination with this approach gives better results but it is more time-consuming.

The third approach is analytical and will be described here for first time ever. It is based on a contour integration. This is the most precise and most rapid technique.

6.1. Average anisotropic vertical factors to a vertical surface

For a vertical rectangle (wall) with horizontal dimension ***a*** and height ***d*** (Fig. 7) the anisotropic vertical factor for the circular segment $\boldsymbol{A_1}$ could be estimated using contour integration of Eq. (A.1):

$$AVF_{A_1\to rect} = \frac{1}{\pi a d}\int_0^d\int_0^a AVF_{A_1\to point}\,dxdh \tag{35}$$

$$AVF_{A_1\to rect} = \frac{1}{2\pi a d}\int_0^d\int_0^a\left(\frac{3}{3+2b}arctg\frac{h}{x}+\frac{2b}{3+2b}\left(1-\frac{x}{\sqrt{x^2+h^2}}\right)\right)dxdh \tag{36}$$

The solved double integral is included as Eq. (A.9) in the Appendix Table A.3.

By analogy we estimate the average AVF of the basic sectors $\boldsymbol{A_2}$, $\boldsymbol{B_1}$ and $\boldsymbol{B_2}$ resulting in the equations described in the Appendix Table A.3. The receiving surface is a vertical rectangle with dimensions ***a*** × ***d***, the distance to the further parallel directly opposite rectangle is ***c***.

6.2. Derivative average anisotropic vertical factors to a vertical surface

With combinations of sums and differences of Eq. (A.9) to (A.12), we can estimate the value of the sky view factor of each visible part of sky, if it is hidden by an orthogonally orientated horizontal or vertical surface.

Eq. (37) estimates the anisotropic vertical factor from a vertical rectangular opening (***c*** × ***d***) to a perpendicular vertical rectangle (***a*** × ***d***) with a common vertical edge ***d*** (Fig. 7 and Fig. 9a).

$$\begin{aligned}
&AVF_{A_1\to rect} - AVF_{B_1\to rect} = \\
&= \frac{3}{(3+2b)}\cdot\frac{1}{2\pi a d}\left(\begin{array}{l} ad.\mathrm{arctg}\frac{d}{a}+cd.\mathrm{arctg}\frac{d}{c}-d\sqrt{a^2+c^2}.\mathrm{arctg}\frac{d}{\sqrt{a^2+c^2}}- \\ -\frac{a^2}{4}\ln\frac{(a^2+c^2)(a^2+d^2)}{a^2(a^2+c^2+d^2)}-\frac{c^2}{4}\ln\frac{\left(a^2+c^2\right)\left(c^2+d^2\right)}{c^2\left(a^2+c^2+d^2\right)}+\frac{d^2}{4}\ln\frac{(a^2+d^2)(c^2+d^2)}{d^2(a^2+c^2+d^2)}\end{array}\right)+ \\
&+\frac{2b}{(3+2b)}\cdot\frac{1}{2\pi a d}\left(\begin{array}{l} d\left(\frac{\sqrt{a^2+c^2+d^2}}{2}-\frac{\sqrt{a^2+d^2}}{2}-\frac{\sqrt{c^2+d^2}}{2}+c+a+\frac{d}{2}-\sqrt{a^2+c^2}\right)+ \\ +\frac{a^2+c^2}{2}\ln\frac{\sqrt{a^2+c^2+d^2}+d}{\sqrt{a^2+c^2}}-\frac{c^2}{2}\ln\frac{\sqrt{c^2+d^2}+d}{c}-\frac{a^2}{2}\ln\frac{\sqrt{a^2+d^2}+d}{a}\end{array}\right)
\end{aligned} \tag{37}$$

Solar Energy 95 (2013) DOI: http://dx.doi.org/10.1016/j.solener.2013.01.021

Equation (38) gives in result one half of the anisotropic vertical factor from a horizontal rectangular opening (***a*** × ***c***) to a perpendicular vertical rectangle (***a*** × ***d***) with a common horizontal edge ***a*** (Fig. 7 and Fig. 9b).

$$AVF_{A_2\to rect} - AVF_{B_2\to rect} =$$

$$= \frac{3}{(3+2b)}\cdot\frac{1}{2\pi ad}\left(\begin{array}{l} ac.\mathrm{arctg}\frac{a}{c} + ad.\mathrm{arctg}\frac{a}{d} - a\sqrt{c^2+d^2}.\mathrm{arctg}\frac{a}{\sqrt{c^2+d^2}} + \\ +\frac{a^2}{4}\ln\frac{(a^2+c^2)(a^2+d^2)}{a^2(a^2+c^2+d^2)} - \frac{c^2}{4}\ln\frac{(a^2+c^2)(c^2+d^2)}{(a^2+c^2+d^2)c^2} - \frac{d^2}{4}\ln\frac{(a^2+d^2)(c^2+d^2)}{d^2(a^2+c^2+d^2)} \end{array}\right) + \quad (38)$$

$$+\frac{2b}{(3+2b)}\cdot\frac{1}{2\pi ad}\left(\begin{array}{l} \frac{d}{2}\left(\sqrt{a^2+d^2}+\sqrt{c^2+d^2}-d-\sqrt{a^2+c^2+d^2}\right) + ac.\mathrm{arctg}\frac{ad}{c\sqrt{a^2+c^2+d^2}} + \\ +\frac{a^2}{2}\ln\frac{\sqrt{a^2+d^2}+d}{a} - \frac{a^2-c^2}{2}.\ln\frac{\sqrt{a^2+c^2+d^2}+d}{\sqrt{a^2+c^2}} - -\frac{c^2}{2}\ln\frac{\sqrt{c^2+d^2}+d}{c} \end{array}\right)$$

Equation (39) gives in result one half of the anisotropic vertical factor from a vertical rectangular opening (***a*** × ***d***) to a directly opposite vertical rectangle (***a*** × ***d***) with a horizontal distance ***c*** between them (Fig. 7 and Fig. 9c).

$$AVF_{B_1\to rect} + AVF_{B_2\to rect} =$$

$$= \frac{3}{(3+2b)}\cdot\frac{1}{2\pi ad}\left(\begin{array}{l} d\sqrt{a^2+c^2}.\mathrm{arctg}\frac{d}{\sqrt{a^2+c^2}} + a\sqrt{c^2+d^2}.\mathrm{arctg}\frac{a}{\sqrt{c^2+d^2}} \\ -cd.\mathrm{arctg}\frac{d}{c} - ac.\mathrm{arctg}\frac{a}{c} + \frac{c^2}{2}\ln\frac{(a^2+c^2)(c^2+d^2)}{(a^2+c^2+d^2)c^2} \end{array}\right) + \quad (39)$$

$$+\frac{2b}{(3+2b)}\cdot\frac{1}{2\pi ad}\left(\begin{array}{l} d\left(\sqrt{a^2+c^2}-c\right) - ac.\mathrm{arctg}\frac{ad}{c\sqrt{a^2+c^2+d^2}} \\ -c^2\ln\frac{\sqrt{a^2+c^2+d^2}+d}{\sqrt{a^2+c^2}} + c^2\ln\frac{\sqrt{c^2+d^2}+d}{c} \end{array}\right)$$

Again the resulting Eqs. (37) – (39) for averaged anisotropic vertical factors include two parts:

(a) The isotropic part multiplied by **3/(3+2*b*)** is the averaged isotropic view factor for the specific sector.

(b) The anisotropic part multiplied by **2*b*/(3+2*b*)** is an anisotropic correction of the isotropic view factor.

Thus the listed equations for averaged anisotropic factors for ***b*=0** could be used for these irradiance models, where the background component of the diffuse irradiance is uniform (isotropic).

The isotropic part of Eq. (37) and (39) after normalization (***X=a/d; Y=c/d; H=c/a; W=d/a***) and some small transformations leads to the already known configuration factors in radiative heat transfer calculations (**Cengel, 2006**) between aligned parallel rectangles – Eq. (40) or two perpendicular rectangles with a common edge – Eq. (41):

Solar Energy 95 (2013) DOI: http://dx.doi.org/10.1016/j.solener.2013.01.021

$$F_{i\to j}=\frac{2}{\pi XY}\left(\begin{array}{l}\ln\sqrt{\frac{(1+X^2)(1+Y^2)}{1+X^2+Y^2}}+X\sqrt{1+Y^2}\,\mathrm{arctg}\frac{X}{\sqrt{1+Y^2}}+\\+Y\sqrt{1+X^2}\,\mathrm{arctg}\frac{Y}{\sqrt{1+X^2}}-X\,\mathrm{arctg}\,X-Y\,\mathrm{arctg}\,Y\end{array}\right) \tag{40}$$

$$F_{i\to j}=\frac{2}{\pi W}\left(\begin{array}{l}W\,\mathrm{arctg}\,W+H\,\mathrm{arctg}\,H-\sqrt{H^2+W^2}\,\mathrm{arctg}\frac{1}{\sqrt{H^2+W^2}}+\\+\frac{1}{4}\ln\left(\frac{(1+W^2)(1+H^2)}{1+W^2+H^2}\left(\frac{W^2(1+W^2+H^2)}{(1+W^2)(1+H^2)}\right)^{W^2}\left(\frac{H^2(1+W^2+H^2)}{(1+W^2)(1+H^2)}\right)^{H^2}\right)\end{array}\right) \tag{41}$$

All equations in Appendix Tables A.1 to A.4 can be normalized by analogy if necessary.

6.3. Average anisotropic factors from infinitely high or long shading surfaces to a vertical surface

Using a similar approach as in Section 6.1 but with a single integral instead because of the infinite height of the obstructing wall we come to Eq. (42) to estimate the average anisotropic factor for section $\boldsymbol{C}_1$. Its solution is Eq. (A.13) in Appendix Table A.4.

$$AVF_{C_1\to rect}=\frac{3\pi+4b}{4\pi a(3+2b)}\int_0^a\frac{x}{\sqrt{x^2+c^2}}dx \tag{42}$$

The following equations (A.14)–(A.16) are for the next studied sky sections $\boldsymbol{C}_2$, $\boldsymbol{D}_1$ and $\boldsymbol{D}_2$. There is a relationship between these equations and some equations in table A.3. For example the Eq. (A.13) corresponds to Eq. (A.11) for an infinitely large value of $\boldsymbol{d}$ ($\boldsymbol{d}\to\infty$). The Eq. (A.15) corresponds to Eq. (A.12), but for an infinitely large value of $\boldsymbol{a}$ ($\boldsymbol{a}\to\infty$).

In Eqs. (A.13) to (A.16) we can notice again the isotropic part, multiplied by **3/(3+2*b*)** and its anisotropic correction, multiplied by **2*b*/(3+2*b*)**.

7. RELATIONS BETWEEN ANISOTROPIC VIEW FACTORS. ANISOTROPIC FACTOR ALGEBRA

From the definition of the average anisotropic view factors to surfaces and their meaning we could formulate some fundamental relations between them.

7.1. Superposition rules

Two superposition rules could be defined for anisotropic view factors to surfaces.

Rule 1: The product of the anisotropic view factor $\boldsymbol{F_{i\to j}}$ from an opening ***i*** to surface ***j*** and the area $\boldsymbol{A_j}$ of surface ***j*** is equal to the sum of the products of the anisotropic view factors from opening ***i*** to the parts of surface ***j*** and their areas – Eq. (43).

$$F_{i\to j}A_j=\sum_{k=1}^{N}F_{i\to j_k}A_{j_k} \tag{43}$$

Rule 2: The anisotropic view factor $\boldsymbol{F_{i\to j}}$ from an opening ***i*** to surface ***j*** is equal to the sum of the anisotropic view factors from the parts of opening ***i*** to the surface ***j*** – Eq. (44).

Solar Energy 95 (2013) DOI: http://dx.doi.org/10.1016/j.solener.2013.01.021

$$F_{i\to j} = \sum_{k=1}^{N} F_{i_k \to j} \tag{44}$$

Both superposition rules can help to estimate the anisotropic view factors which cannot be evaluated directly.

7.2. Summation rule

The sum of the anisotropic factors from all sky sectors to an inclined surface must equal a maximum value, specific for any angle of inclination. This maximum value can be estimated with Eq. (2) by Steven about the ratio between the diffuse irradiance on inclined surface under unobstructed sky and horizontal diffuse irradiance, which we reformulated as a ratio between the background components of both mentioned diffuse irradiances – sloped and horizontal.

For a vertical surface this maximum value is given by Eq. (16) and is $(3\pi+4b)/[2\pi(3+2b)]$. For a faced up horizontal surface the maximum value is 1.

7.3. Reciprocity relation for some anisotropic view factors

A reciprocity relation for configuration factors of two isotropic emitting surfaces exists in radiative heat transfer theory. It allows the calculation of a view factor from the knowledge of the other. The reciprocity relation for anisotropic view factors looks similar – Eq. (45). The small difference is because of the different definitions of both types of factors.

$$A_k F_{i\to k} = A_i F_{k\to i} \tag{45}$$

The isotropic parts of the derivative average anisotropic view factors – Eqs. (37) and (39), and also (A.13)–(A.15) satisfy the reciprocity relation. It can be proved analytically that the anisotropic parts of the factors are related in agreement with Eq. (45) in these 4 cases:

- two vertical perpendicular rectangular openings with a common vertical edge – Eq. (37);
- two directly opposite vertical parallel rectangular openings with equal dimensions and areas – Eq. (39);
- two directly opposite vertical parallel infinitely high rectangular openings with equal or different width – Eq. (A.13);
- two vertical perpendicular infinitely high rectangular openings with equal or different width – Eq. (A.14).

Thus in these four cases the anisotropic vertical view factors as combination of isotropic and anisotropic parts satisfy the reciprocity relation.

In spite of this the reciprocity relation is not correct for openings with different heights which show sky areas with different sky radiance.

7.4. Anisotropic factor algebra, examples

The described rules and relations – Eq. (43) to (45) form base of new Anisotropic Factor Algebra. It is intended to be an anisotropic sky version of the Configuration Factor Algebra by **Howell (2010)**.

Using the listed relations new anisotropic view factors can be computed from a set of known factors. Let us check this possibility with some exemplary configurations of vertical perpendicular surfaces with equal height in Fig. 12 and to estimate their ***AVF***.

Solar Energy 95 (2013) DOI: http://dx.doi.org/10.1016/j.solener.2013.01.021

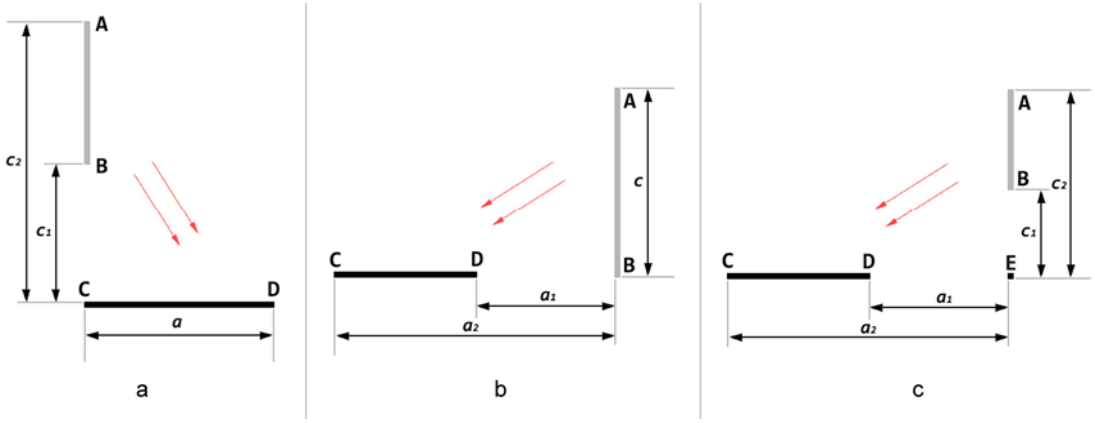

Fig. 12. Exemplary configurations of vertical perpendicular rectangles with equal height – plan view

Let us name the average ***AVF*** from the basic sky sector A_1 to a vertical rectangle with width ***a*** and height ***d*** with the shorter $A_1(a, d)$, estimated with Eq. (A.9); and the average ***AVF*** from the basic sky sector B_1 to a vertical rectangle with width ***a***, distance ***c*** to the opposite corner and height ***d*** with the shorter $B_1(a, c, d)$, estimated with Eq. (A.11). The order and meaning of parameters are important and they cannot be exchanged.

7.4.1. Example 1

The first example includes two vertical perpendicular rectangles with equal height ***d*** and horizontal projections **AB** and **CD**, as they are displayed on Fig. 12a. According superposition rule 2 the sum of $AVF_{AB\to CD}$ and $AVF_{BC\to CD}$ is equal to $AVF_{AC\to CD}$. This way we could estimate $AVF_{AB\to CD}$ from the values of $AVF_{AC\to CD}$ and $AVF_{BC\to CD}$:

$$AVF_{AB\to CD} = AVF_{AC\to CD} - AVF_{BC\to CD} = \left[A_1(a,d) - B_1(a,c_2,d)\right] - \left[A_1(a,d) - B_1(a,c_1,d)\right] \quad (46)$$

$$AVF_{AB\to CD} = B_1(a,c_1,d) - B_1(a,c_2,d) \quad (47)$$

7.4.2. Example 2

The second example includes two vertical perpendicular rectangles with equal height ***d*** and horizontal projections **AB** and **CD**, as they are displayed on Fig. 12b – a configuration, which is opposite to the previous example on Fig. 12a. According the reciprocity relation and using the previous example:

$$(a_2 - a_1)d.AVF_{AB\to CD} = cd.AVF_{CD\to AB} \quad (48)$$

$$AVF_{AB\to CD} = AVF_{CD\to AB}.\frac{c}{a_2 - a_1} = \frac{c}{a_2 - a_1}\left[B_1(c,a_1,d) - B_1(c,a_2,d)\right] \quad (49)$$

7.4.3. Example 3

The third example includes two vertical perpendicular rectangles with equal height ***d*** and horizontal projections **AB** and **CD**, as they are displayed on Fig. 12c. In this case we compute the new ***AVF*** using again the superposition rule 2 and the result from the example 2.

$$AVF_{AB\to CD} = AVF_{AE\to CD} - AVF_{BE\to CD} = AVF_{CD\to AE}.\frac{c_2}{a_2 - a_1} - AVF_{CD\to BE}.\frac{c_1}{a_2 - a_1} \quad (50)$$

$$AVF_{AB\to CD} = \frac{c_2}{a_2 - a_1}\left[B_1(c_2,a_1,d) - B_1(c_2,a_2,d)\right] - \frac{c_1}{a_2 - a_1}\left[B_1(c_1,a_1,d) - B_1(c_1,a_2,d)\right] \quad (51)$$

More configurations of vertical surfaces – opposite and perpendicular, with equal or different heights need to be studied to estimate their ***AVF***.

Solar Energy 95 (2013) DOI: http://dx.doi.org/10.1016/j.solener.2013.01.021

8. DISCUSSION AND CONCLUSION

This work modifies the existing anisotropic irradiance model of Muneer in order to predict the background sky diffuse radiance at any point of the sky and expands it with a new definition of anisotropic view factor. A set of basic relations between anisotropic view factors are defined and several cases of orthogonally obstructed sky with finite or infinitely long or high surfaces are presented which together form base of a new anisotropic factor algebra.

This could help to estimate background diffuse irradiance under clear and overcast skies in urban environment – onto the building surfaces, onto the building facades in the urban street canyons and the surfaces under horizontal shading devices.

The limits of the resulting equations in the Appendix Tables A.3 and A.4 come from the specific reciprocal positions of the studied surfaces (receiving walls and openings) which must be parts of a rectangular cuboid. Using the relations of anisotropic factor algebra new anisotropic view factors can be computed from the set of known factors in the Appendix A. The equations in the Appendix Tables A.1 and A.2 could be used to expand the current model with orthogonal surfaces in general positions.

The anisotropic factor algebra still needs a lot of efforts to be expanded with anisotropic factors for other geometries. The limits of the reciprocity relation also have to be studied more.

APPENDIX

Table A.1. Equations for estimation of anisotropic vertical factors of the basic sky sectors to a point of a vertical wall.

Image of basic sector	Equation	Equation No
A_1 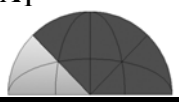	$AVF_{A_1\to point}=\frac{3}{3+2b}\left(\frac{1}{2\pi}\operatorname{arctg}\frac{h}{x}\right)+\frac{2b}{3+2b}.\frac{1}{2\pi}\left(1-\frac{x}{\sqrt{x^2+h^2}}\right)$	(A.1)
A_2 	$AVF_{A_2\to point}=\frac{3}{3+2b}\left(\frac{1}{2\pi}\operatorname{arctg}\frac{x}{h}\right)+\frac{2b}{3+2b}\left(\frac{1}{2\pi}.\frac{x}{\sqrt{x^2+h^2}}\right)$	(A.2)
B_1 	$AVF_{B_1\to point}=\frac{3}{3+2b}\left(\frac{1}{2\pi}.\frac{x}{\sqrt{x^2+c^2}}\operatorname{arctg}\frac{h}{\sqrt{x^2+c^2}}\right)+$ $+\frac{2b}{3+2b}.\frac{1}{2\pi}\left(\frac{x}{\sqrt{x^2+c^2}}-\frac{x}{\sqrt{x^2+c^2+h^2}}\right)$	(A.3)
B_2 	$AVF_{B_2\to point}=\frac{3}{3+2b}\left(\frac{1}{2\pi}.\frac{h}{\sqrt{c^2+h^2}}\operatorname{arctg}\frac{x}{\sqrt{c^2+h^2}}\right)+$ $+\frac{2b}{3+2b}\left(\frac{1}{2\pi}.\frac{xh^2}{(c^2+h^2)\sqrt{x^2+c^2+h^2}}\right)$	(A.4)

Solar Energy 95 (2013) DOI: http://dx.doi.org/10.1016/j.solener.2013.01.021

Table A.2. The anisotropic view factors from a sky partially obstructed by infinitely high vertical walls or infinitely long urban canyon to a point of a vertical surface

Image of basic section	Equation	Equation No
$h \to \infty$ 	$AVF_{C_1 \to point} = \frac{3}{3+2b}.\frac{x}{4\sqrt{x^2+c^2}} + \frac{2b}{3+2b}.\frac{x}{2\pi\sqrt{x^2+c^2}}$	(A.5)
$h \to \infty$ 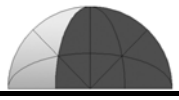	$AVF_{C_2 \to point} = \frac{3}{3+2b}.\frac{1}{4}\left(1-\frac{x}{\sqrt{x^2+c^2}}\right) + \frac{2b}{3+2b}.\frac{1}{2\pi}\left(1-\frac{x}{\sqrt{x^2+c^2}}\right)$	(A.6)
$x \to \infty$ 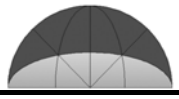	$AVF_{D_1 \to point} = \frac{3}{3+2b}\left(\frac{h}{2\sqrt{c^2+h^2}}\right) + \frac{2b}{3+2b}\left(\frac{h^2}{\pi(c^2+h^2)}\right)$	(A.7)
$x \to \infty$ 	$AVF_{D_2 \to point} = \frac{3}{3+2b}.\frac{1}{2}\left(1-\frac{h}{\sqrt{c^2+h^2}}\right) + \frac{2b}{3+2b}\left(\frac{c^2}{\pi(c^2+h^2)}\right)$	(A.8)

Table A.3. Equations for estimation of average anisotropic view factors of the basic sectors to a vertical rectangle

Image of basic sector	Equation	Equation No
A_1 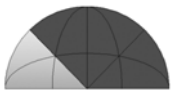	$AVF_{A_1 \to rect} = \frac{3}{3+2b}.\frac{1}{2\pi ad}\left(ad.\text{arctg}\frac{d}{a} - \frac{a^2}{4}\ln\frac{a^2+d^2}{a^2} + \frac{d^2}{4}\ln\frac{a^2+d^2}{d^2}\right) + \frac{2b}{3+2b}.\frac{1}{2\pi ad}\left(ad - \frac{d}{2}\left(\sqrt{a^2+d^2}-d\right) - \frac{a^2}{2}\ln\frac{\sqrt{a^2+d^2}+d}{a}\right)$	(A.9)
A_2 	$AVF_{A_2 \to rect} = \frac{3}{3+2b}.\frac{1}{2\pi ad}\left(ad.\text{arctg}\frac{a}{d} + \frac{a^2}{4}\ln\frac{a^2+d^2}{a^2} - \frac{d^2}{4}\ln\frac{a^2+d^2}{d^2}\right) + \frac{2b}{3+2b}.\frac{1}{2\pi ad}\left(\frac{d}{2}\left(\sqrt{a^2+d^2}-d\right) + \frac{a^2}{2}\ln\frac{\sqrt{a^2+d^2}+d}{a}\right)$	(A.10)
B_1 	$AVF_{B_1 \to rect} = \frac{3}{(3+2b)}.\frac{1}{2\pi ad}\left(\begin{array}{l} d\sqrt{a^2+c^2}.\text{arctg}\frac{d}{\sqrt{a^2+c^2}} - cd.\text{arctg}\frac{d}{c} - \\ -\frac{a^2}{4}\ln\frac{a^2+c^2+d^2}{a^2+c^2} + \frac{c^2}{4}\ln\frac{\left(a^2+c^2\right)\left(c^2+d^2\right)}{c^2\left(a^2+c^2+d^2\right)} + \\ +\frac{d^2}{4}\ln\frac{a^2+c^2+d^2}{c^2+d^2} \end{array}\right) + \frac{2b}{3+2b}.\frac{1}{2\pi ad}\left(\begin{array}{l} d\left(\sqrt{a^2+c^2}-c+\frac{\sqrt{c^2+d^2}}{2}-\frac{\sqrt{a^2+c^2+d^2}}{2}\right) - \\ -\frac{a^2+c^2}{2}\ln\frac{\sqrt{a^2+c^2+d^2}+d}{\sqrt{a^2+c^2}} + \frac{c^2}{2}\ln\frac{\sqrt{c^2+d^2}+d}{c} \end{array}\right)$	(A.11)

Solar Energy 95 (2013) DOI: http://dx.doi.org/10.1016/j.solener.2013.01.021

B_2 	$AVF_{B_2\to rect} =$ $= \frac{3}{3+2b}\cdot\frac{1}{2\pi ad}\left(\begin{array}{l} a\sqrt{c^2+d^2}.\text{arctg}\frac{a}{\sqrt{c^2+d^2}} - ac.\text{arctg}\frac{a}{c} + \frac{a^2}{4}\ln\frac{a^2+c^2+d^2}{a^2+c^2} + \\ + \frac{c^2}{4}\ln\frac{(a^2+c^2)(c^2+d^2)}{(a^2+c^2+d^2)c^2} - \frac{d^2}{4}\ln\frac{a^2+c^2+d^2}{c^2+d^2} \end{array}\right) +$ $+ \frac{2b}{3+2b}\cdot\frac{1}{2\pi ad}\left(\begin{array}{l} \frac{d}{2}\left(\sqrt{a^2+c^2+d^2}-\sqrt{c^2+d^2}\right) - ac.\text{arctg}\frac{ad}{c\sqrt{a^2+c^2+d^2}} + \\ + \frac{a^2-c^2}{2}.\ln\frac{\sqrt{a^2+c^2+d^2}+d}{\sqrt{a^2+c^2}} + \frac{c^2}{2}\ln\frac{\sqrt{c^2+d^2}+d}{c} \end{array}\right)$	(A.12)

Table A.4. Average anisotropic vertical factors from a sky partially obstructed by infinitely high vertical walls or infinitely long urban canyon to a vertical surface

Image of basic section	Equation	Equation No
$d \to \infty$ 	$AVF_{C_1\to rect} = \frac{3}{3+2b}\left(\frac{\sqrt{a^2+c^2}-c}{4a}\right) + \frac{2b}{3+2b}\left(\frac{\sqrt{a^2+c^2}-c}{2\pi a}\right)$	(A.13)
$d \to \infty$ 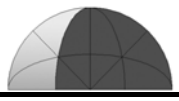	$AVF_{C_2\to rect} = \frac{3}{3+2b}\left(\frac{a+c-\sqrt{a^2+c^2}}{4a}\right) + \frac{2b}{3+2b}\left(\frac{a+c-\sqrt{a^2+c^2}}{2\pi a}\right)$	(A.14)
$a \to \infty$ 	$AVF_{D_1\to rect} = \frac{3}{3+2b}\left(\frac{\sqrt{c^2+d^2}-c}{2d}\right) + \frac{2b}{3+2b}.\frac{1}{\pi}\left(1-\frac{c}{d}\text{arctg}\frac{d}{c}\right)$	(A.15)
$a \to \infty$ 	$AVF_{D_2\to rect} = \frac{3}{3+2b}\left(\frac{c+d-\sqrt{c^2+d^2}}{2d}\right) + \frac{2b}{3+2b}\left(\frac{c}{\pi d}\text{arctg}\frac{d}{c}\right)$	(A.16)

References

Brunger, A. P, & Hooper F. C., 1993, Anisotropic sky radiance model based on narrow field of view measurements of shortwave radiance. Solar Energy, Vol. 51, No. 1, pp. 53-64

Cengel, Y., 2006, Heat and Mass Transfer: A Practical Approach, third ed. McGraw-Hill

Clarke P., Muneer T., Davidson A. and Kubie J., 2007, Models for the estimation of building integrated photovoltaic systems in urban environments, Proc. IMechE Vol. 222 Part A: J. Power and Energy

Evseev E. G. & Kudish A. I, 2009, The assessment of different models to predict the global solar radiation on a surface tilted to the south, Solar Energy 83, pp. 377–388

Hay, J.E., 1979, Calculation of monthly mean solar radiation for horizontal and inclined surfaces. Solar Energy 23, 301.

Hay, J.E. and Davies, J.A., 1980, Calculation of the solar radiation incident on an inclined surface, Proc. First Canadian Solar Radiation Data Workshop. Ministry of Supply and Services, Canada, p. 59.

Solar Energy 95 (2013) DOI: http://dx.doi.org/10.1016/j.solener.2013.01.021

Hay, J.E. and McKay, D.C., 1988, Calculation of Solar Irradiances for Inclined Surfaces: Verification of Models which Use Hourly and Daily Data. IEA Task IX Final Report, Atmospheric Environment Service, Downsview, Canada.

Hofierka J. & Šúri M., 2002, The solar radiation model for Open source GIS: implementation and applications, Proceedings of the Open source GIS - GRASS users conference 2002 - Trento, Italy

Howell, J., 2010, A catalog of Radiation Heat Transfer – Configuration Factors, 3rd edition, http://www.engr.uky.edu/rtl/Catalog/

Ivanova, S., 2011, Estimation of solar radiation for buildings with complex architectural layouts. International Conference Solaris - 2011, Brno, Czech Republic

Kondratyev, K.Ya., 1969, Radiation in the Atmosphere. Academic Press, New York.

Loutzenhiser P. G., Manz H., Felsmann C., Strachan P. A., Frank T., Maxwell G. M., 2007, Empirical validation of models to compute solar irradiance on inclined surfaces for building energy simulation, Solar Energy 81, pp. 254-267

McArthur B, Hay J. E., 1981, A Technique for Mapping the Distribution of Diffuse Solar Radiation over the Sky Hemisphere, J. Applied Meteorology 20, 421-429

Moon, P. & Spencer, D. E., 1942, Illumination from a non-uniform sky. Trans. Illum. Eng. Soc., London, 37, pp. 707-725

Muneer, T., 1990, Solar radiation model for Europe. Building Serv. Eng. Res. Technol, 11(4), 153-163

Muneer, T., 2004, Solar radiation and daylight models, second ed. Oxford; Burlington, MA: Elsevier Butterworth Heinemann

Muneer, T., Zhang, X., 2002, A new method for correcting shadow band diffuse irradiance data, ASME Journal of Solar Energy Engineering, 124 (1). pp. 34-43

Perez R., Seals R. and Michalsky J., 1993, All-weather model for sky luminance distribution – Preliminary configuration and validation, Solar Energy 50, pp. 235-245

Steven M. D. & Unsworth M. H., 1980, The angular distribution and interception of diffuse solar radiation below overcast skies, *Quart. J. R. Met.* SOC.(1 980), 106, pp. 57-61

Usher, J.R. and Muneer, T., 1989, Case studies in solar radiation modelling. Math. Comput. Model. 12, 1155.

Wlodarczyk D. & Nowak H., 2009, Statistical analysis of solar radiation models onto inclined planes for climatic conditions of Lower Silesia in Poland, Archives of civil and mechanical engineering, Vol. IX 2009 No. 2